

On the complex zonality in grandite garnets and implications

T. I. IVANOVA, A. G. SHTUKENBERG, Yu. O. PUNIN, O. V. FRANK-KAMENETSKAYA AND P. B. SOKOLOV

Department of Crystallography, Saint-Petersburg State University, University Emb. 7/9, 199034 Saint-Petersburg, Russia

ABSTRACT

The available data on compositional zoning in grossular–andradite (grandite) garnets occurring at different scales, mainly due to the variations of their Fe^{3+}/Al ratios, and the hypotheses on the origin of this zoning are reviewed. Four zoned crystals of grandites showing different optical properties have been studied by means of X-ray diffraction. Optical and structural studies suggest three superimposed scales of Fe^{3+}/Al zonality along [110]. The drastic change of the structural characteristics from sample to sample correlates with the change of their optical patterns. The superfine oscillatory zoning has been described in terms of irregular interstratified structures with a high degree of segregation. The self-affinity of zoning at different scales testify to the possible origin of the zonality due to the non-linear dynamics at the growth front. The wide variation of the layer compositions revealed by the modelling of the X-ray diffraction profiles seems to contradict the hypothesis of unmixing in grandite garnets.

KEYWORDS: garnet, grandite, zoning.

Introduction

GROSSULAR–ANDRADITE (grandite) garnets usually show intracrystalline zonality of different types which has been described in a number of papers (Lessing and Standish, 1973; Vlasova *et al.*, 1975; Murad, 1976; Hirai *et al.*, 1982; Hirai and Nakazawa, 1982, 1986a,b; Akizuki *et al.*, 1984; Jamtveit, 1991; Jamtveit *et al.*, 1993, 1995). It has been shown that the zones in grandites differ mainly in their Fe^{3+}/Al ratios but the distribution of trace elements (for instance, Ti, As, Mn) can also be inhomogeneous (Jamtveit *et al.*, 1995). Besides, the changes in Al/Fe ordering may result in the zonality which is visible with a polarising microscope and is due to the difference in either the birefringence or the direction of extinction between the zones (Shtukenberg *et al.*, 1996). Table I summarises the data available on the compositional zonality in grandites.

The compositional changes can be either continuous or discrete, with sharp boundaries of the zones. In both the cases, either periodic or non-periodic changes can occur. In non-periodic zonality the thickness of zones can vary from a few μm to a few centimetres. Two scales of oscillating compositional variations can co-exist in a crystal; a coarse one with a thickness from

tens to hundreds of μm , and a fine one with a thickness of tenths to tens of μm . Moreover, the birefringent major zones with intermediate composition in the grossular–andradite series usually contain the fine zones. At the same time, the isotropic coarse zones, with compositions close to those of the end-members of the series, are usually homogeneous. As a rule, the complex oscillating zonality is parallel to the growth front which in most cases corresponds to the faces (110) of a dodecahedron. In some cases this zonality is accompanied by the lamellar texture with a variable direction of alternation relative to the growth front. The thickness of the lamellae can vary from a few, up to tens of μm . Some of them have a wavy shape.

According to the scale of zonality, various methods of its study are commonly used. Electron probe microanalysis and optical microscopy are suitable for the study of zonality with the thickness of zones more than tens of μm . In the case of fine zonality other electron microscopy (EM) techniques (scanning, transmission or analytical electron microscopy) can be additionally used. Optical diffraction (OD) is useful for the study of strictly periodic zonality if the zones differ in their optical properties and have the

TABLE 1. The types of zonality and lamellae texture of grandite garnets

Sample N	Type	h^0 , μm	$x^{\text{Fe}} = \text{Fe}/(\text{Fe}+\text{Al})$, mol. fraction	OP	Direction of alternation ^{b)}	Origin	Methods	Reference	Arrangement of zones and lamellae within the sample
1		1-200	0.91-0.97	I	[110]	Cyclic variations of temperature and composition of hydrothermal solutions	EPMA, OM	Murad, 1976	
		5-50	0.55-0.72	B	[110]				
2		5-50	1.0	I	[110]	Rapid changes in chemical composition of hydrothermal solutions	OM, EPMA	Lessing and Standish, 1973	
		5-28	0	B					
3		5-28	0.47-0.56	?	[110]	?	EPMA	Vlasova <i>et al.</i> , 1975	
			0.76						
4		10-30	0.98	?	[110]	Variations of growth conditions	SEM, EPMA	Jamtveit <i>et al.</i> , 1995	
			0.6						
5	a	100-200	1.0	I		Variations of growth conditions	SEM, EPMA	Jamtveit <i>et al.</i> , 1993	Zones of type b alternate within the birefringent zones of type a
	b	10-20	0.8	B	[110]				
6		5-8	0.92			Variations of growth conditions	SEM, EPMA	Jamtveit, 1991	Zones of type b alternate within the Al-rich birefringent zones of type a
		2-3	0.72						
7	a	5-20	0.55-0.6	B		Nonlinear growth dynamics at the crystal-solution interface in the presence of a miscibility gap	SEM, EPMA	Jamtveit, 1991	Zones of type b alternate within the Al-rich birefringent zones of type a
	b	0.1-2	0.1-0.15	B	[110]				
8	a	2-10	0.12±0.03	I		Postgrowth exsolution	SEM, EPMA	Jamtveit, 1991	Zones of type b alternate within the Al-rich birefringent zones of type a
	b	0.5-2	0.65-0.7	B					
9	a	160	0.68±0.03	I		Twinning	OD, OM	Hirai and Nakazawa, 1982	Zones of type b (twins with constant thickness) alternate within the birefringent zones of type a
	b	40	0.5*	B	[110]				
9	c	0.1	?			Growth zonality	SEM	Akizuki <i>et al.</i> , 1984	Flat lamellae of type c coexist with the wavy lamellae of type d within the birefringent zones of type a
	d	1-0.2	0.9**	B	close to [501]				
9	a	8-10	0.9**	I		Growth zonality	OM, SEM	Akizuki <i>et al.</i> , 1984	Zones of type b alternate within some zones of type a
	b	10-15	0.83**	?	[110]				

TABLE 1 (contd)

10***	a	10-90	?	I B	[110]	Compositional changes of solution during growth	OM, SEM, EPMA	Hirai <i>et al</i> , 1982	Flat lamellae of type b alternate within the compositional zones of type a
	b	8-10 2-4	0.98 0.9	I B	varies from nearly perpendicular to nearly parallel to [110]	Postgrowth exsolution			Wavy lamellae of type c cross several compositional zones of type a but can gradually change their orientation and join the lamellae of type b
	c	5-7	?	?					
11***	a	5-10	?	?	Inclined by a few degrees to [110]	Growth zonality	TEM, AEM, SEM	Hirai and Nakazawa, 1986a	The lamellae of type b alternate within the coarse zones of type a. Observed moiré-like texture with the period of appr. 10 µm is considered to occur due to the intersections of the lamellae of types b and c
	b	0.5-0.6 0.1-0.2	0.87 0.78	?					
	c	?	?	?	[110]	Postgrowth exsolution			
12	a	1-30	0.5**	B	[110]	Growth zonality			Lamellae of type b with two equivalent orientations cross the compositional zones of type a
	b	1-5	0.58	B	most likely [100]	Postgrowth exsolution	SEM, OM, EPMA	Hirai and Nakazawa, 1986b	

1/a: thickness of zones or lamellae;
 2/x: composition of zones or lamellae;
 3: growth front is parallel to [110] in all the samples which have dodecahedral habit.
 ?: no information;
 * calculated from the mean composition of the sample and volume proportion of zones;
 ** mean composition of the sample;
 ***the same crystal as No 8.
 Abbreviations: I: isotropic; B: birefringent; OP: optical properties; OM: optical microscopy; EPMA: electron probe microanalysis; SEM: scanning electron microscopy; TEM: transmission electron microscopy; AEM: analytical electron microscopy; OD: optical diffraction

thickness of the order of 1000 Å. With the OD technique the thickness of zones can be properly determined but no information about their composition can be obtained. Although it has a great advantage in revealing fine scale structural details, electron microscopy is a localised method. On the other hand, X-ray diffraction studies permit the determination of average structural characteristics of a crystal. A number of X-ray structural studies of grandites (Novak and Gibbs, 1971; Takeuchi *et al.*, 1982; Lager *et al.*, 1989; Allen and Buseck, 1988; Kingma and Downs, 1989 etc.) have been carried out. However, the diffraction peak profile analysis, which can help in revealing the inhomogeneity of the crystal even at the superfine level (hundreds of angstroms), have not been used up to now. The statistical model of disordered lamellar structures (Drits and Tchoubar, 1990) permits a quantitative description of the inhomogeneity of single crystals with layer defects, intergrowths, fine zonality, exsolution textures etc. (Frank-Kamenetskaya and Ivanova, 1997). We applied this approach to the study of the zoned crystals of grandites. In this paper, the structural models are presented and compared with the optical characteristics of the samples as well as with the results of the studies of the zonality in grandites carried out by the other researches using different techniques.

Theoretical background

Interstratified (or mixed-layered) structures are built from two-dimensional modules (layers) differing in chemical composition as well as in crystal structure. The modules are stacked in a more or less ordered sequence and can occur in any proportion. Irregular alternation of layers, having identical or fairly different two-dimensional cell in the layer plane that allows them to coexist within a coherent domain, perturbs the perfect periodicity of the whole structure in the direction perpendicular to the layer plane. For the quantitative description of the irregular interstratified structures of single crystals we proposed (Frank-Kamenetskaya and Ivanova, 1997) the use of the statistical model (Drits and Tchoubar, 1990) with parameters which characterise a proportion of layers and a motif of their distribution along a certain direction in a coherent domain.

The distribution of layers in a two-component irregular interstratified structure with the factor of short-range order $S = 1$ (i.e. the nature of a layer

depends only on the nature of the preceding layer) can be characterised by two independent statistical parameters: the probability of occurrence of one type of layers (W_1 or $W_2 = 1 - W_1$) and one of the conditional probabilities of finding a j -type layer following an i -type in the stack P_{ij} ($i, j = 1, 2$): $P_{ii} = 1 - P_{ij}$, $P_{ji} = (W_i/W_j)P_{ij}$.

The character of alternation of layers with heights h_1 and h_2 in a two-component (major type of layers — matrix, minor type — admixture) irregular interstratified structure is completely defined by the relationship between the probability of occurrence of admixture layers W_2 ($W_2 < W_1$) and the probability of occurrence of an admixture layer following a layer of the same type P_{22} ($0 \leq P_{22} \leq 1$). If $P_{22} = W_2$ the structure is characterised by a random distribution of layers (totally disordered structure with $S = 0$). In the structure with $P_{22} = 0$ the layers of admixture cannot follow each other. They are distributed among the layers of matrix with maximum possible for the structures with $S = 1$ degree of order (MPDO). The case with $P_{22} = 0$ and $W_1 = W_2$ corresponds to the regular (1:1) mixed-layered structure. When $W_2 > P_{22} > 0$, the alternation of layers in the structure has a tendency to order. The total segregation of each type of layers is characterised by $P_{11} = P_{22} = 1$. The structures with $0 < W_2 < P_{22}$ have a tendency to segregation in layer distribution ($P_{22} > P_{21}$). The degree of segregation can be described by the segregation coefficient $K_s = 1 - (1 - P_{22})/(1 - W_2)$ (Sato, 1965). $K_s = 1$ corresponds to the total segregation of layers, $K_s = 0$ — to the total disorder in layer distribution.

The scale of the structural inhomogeneity of a crystal can be characterised (Ivanova *et al.*, 1994) by the maximum possible thickness of a stack of admixture layers $l = W_2 P_{22} L$ in a coherent domain with the size along the certain direction $L = (W_1 h_1 + W_2 h_2) M$, where M is the total number of layers in a coherent domain. The value of l can vary from the height of single admixture layer in the structures with MPDO up to $L/2$ in the structures with high P_{22} and W_2 values.

The specific type of defects — the fluctuations of layer heights around the mean values h_1 and h_2 — can also occur in a stack of layers that originates from the variations of their composition. It can be assumed (Drits and Tchoubar, 1990) that the fluctuations of layer heights follow a normal Gaussian distribution (with σ_h as a standard deviation of layer height) without long-range correlation among the defects which there-

fore yield a disorder of the second type (Guinier, 1961).

The distinct features of the diffraction patterns of crystals with irregular interstratified structures are that basal reflections form irrational series and usually display a broadening and asymmetry of their profiles. The presence of layer height fluctuations affects the diffraction patterns leading to an extra-broadening of reflections. Their width increases rapidly with 2θ whereas their intensity drops drastically.

The determination of the statistical parameters of mixed-layered structures is carried out by trial and error by simulating the diffraction patterns of the crystals. The intensities of the reflections measured along the direction normal to the layer plane are compared with those calculated for a structural model. This allows rejection of the unreliable models but inevitably leads to the multivariant results. The reliability of models can be increased by bringing the data on crystal structural chemistry into agreement with the chemical microanalytical data for the samples.

Experimental

Samples and their optical patterns

Four grandite crystals from limestone skarns of Mali (West Africa) were kindly provided by Dr J. Zang. They exhibited dodecahedral habit and were 1–3 cm in diameter. Plates normal to (001) were cut from each sample and studied with a polarising microscope and by EPMA (Table 2). The samples displayed different types of optical anomalies and showed complicated optical patterns with two scales of zonality. EPMA carried out with a 'Camscan' microanalyser could not distinguish the composition of fine zones which were clearly resolved in optics. Thus, only the average composition of the major zones was determined.

The internal part of sample 1 contains alternating zones with n_g' or n_p' parallel to the growth front. The Becke effect is clearly seen between the zones which means that they have different compositions (Shtukenberg *et al.*, 1996). In the external part of the sample the orientation of the optical indicatrix varies randomly between zones, but the angle between the corresponding axes of the indicatrix does not exceed 20° . In both internal and external parts of the sample the zones also differ in the birefringence value.

The optical pattern of sample 2 is characterised by the alternation of nearly isotropic and

birefringent zones with a mean thickness ratio of 1:3. In most zones n_g' is parallel to the growth front. According to the data on optical anomalies in grandites (Shtukenberg *et al.*, 1996) together with the results of EPMA it could be concluded that isotropic zones have compositions close to that of grossular, whereas birefringent ones represent intermediate members of the grandite series.

Sample 3 has the highest birefringence among the samples and does not display clear zonality in optics but shows wedge-like subzones adjoining the boundaries of the growth sectors and tapering off to their central parts. Different subzones have similar birefringence values but are distinguished by the direction of extinction (few degrees). The nature of these subzones is not clear but it is likely that they differ in the degree of Al/Fe³⁺ ordering (Shtukenberg *et al.*, 1996).

Sample 4 is close to sample 2 from its optical pattern but, the alternating zones with variable thicknesses have birefringence two orders of magnitude higher. The oscillations of birefringence superimpose on the monotonous increase in birefringence from the centre to the outer part of the sample.

X-ray diffraction measurements

X-ray diffraction patterns of garnet crystals were obtained from the natural (110) faces. The measurements of the intensities of $hh0$ reflections were carried out by θ – 2θ scanning along the [110] direction in a conventional autodiffractometer (Co- K_α radiation) equipped with a graphite monochromator. The width of the slit in front of the detector (0.05 mm) was chosen empirically so that further decrease in the width of the slit did not change the half-width of a reflection any more. The scanning step was 0.01 – $0.02^\circ 2\theta$ and the measurement time of up to 10 sec per point were set depending on the half-width and the intensity of the measured reflections. The thin plate of lead with the hole of 3 mm in diameter was placed over the sample to keep the illuminated area constant. The $K\alpha_2$ radiation contribution was subtracted from the experimental data by the method of Reshinger (Guinier, 1961). A natural single crystal of quartz from the Polar Urals was used as a standard.

The depth at which X-rays diffracted by a sample of garnet are weakened by a factor of 10 was determined to be 15–25 μm , depending on

Table 2. The characteristics of zonality in the studied grandite crystals

Sample N	Coarse zone N	Thickness of coarse zones mm	Growth sector	Colour	$x = \text{Fe}^{2+}/(\text{Fe}^{2+} + \text{Al})$, mol. fraction	Value of birefringence $\Delta \cdot 10^{-7}$		The manifestation of fine zonality in optics	Thickness of fine zones, μm
						Average	Maximal		
1	1	10.5–12.5	<110>	Greenish	0.32–0.38	37	98	Different orientation of the optical indicatrix	100–500
	2	1–2	<110>	From colourless to light green	0.22–0.50	94	180	Different orientation of the optical indicatrix	30–100
2	1	6–7	<110>	From greenish to green	0.13–0.18	374	603	Different value of birefringence	Nearly isotropic zones – 3–5
	2	2–3	<110>	Light green	0.37–0.42	322	516	Different value of birefringence	Birefringent zones – 10–15
3	1	8–9	<110>	Reddish-brown	0.22–0.30	65685	69900	No zonality	–
			<211>			1161	2400		
4	1	5–5.5	<110>	Light brown	0.38–0.47	13071	14300	Different value of birefringence	3–60
			<211>			3995	9600		
	2	1	<110>	Brown	0.44–0.51	17247	19400	Different value of birefringence	
			<211>			–	–		

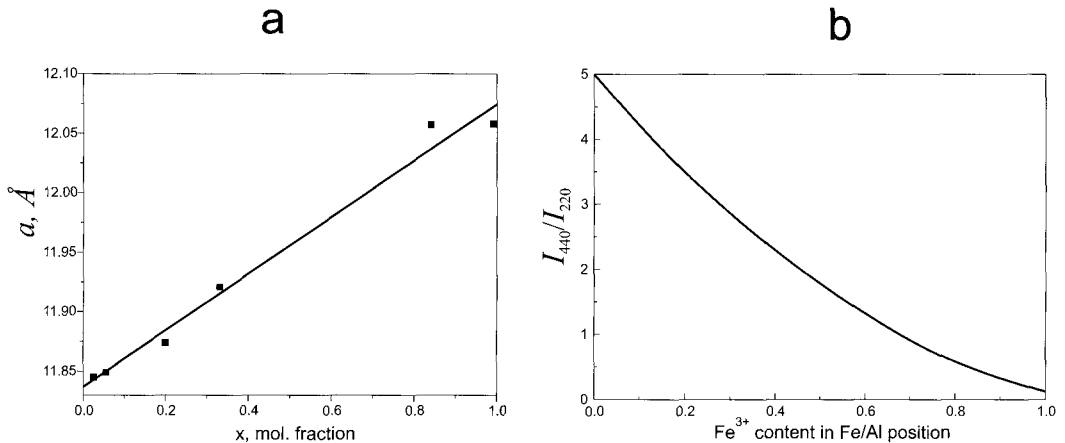


FIG. 1. (a) The lattice constant a (data taken from Novak and Gibbs, 1971; Lager *et al.*, 1989; Allen and Buseck, 1988) as a function of Fe^{3+} fraction x in grandite; (b) the calculated intensity ratio of 440 and 220 reflections as a function of the Fe^{3+} content in the Fe^{3+}/Al crystallographic position in the structure of grandite.

the 2θ angles. This means that the data were collected from the outer zone of a sample.

Simulation of the diffraction patterns

The formalism described by Drits and Tchoubar (1990) was used for calculating the intensity of the wave diffracted by an irregular interstratified system. The atomic co-ordinates in the structure of grandites were taken from Allen and Buseck (1988). The following set of variables were used to define a two-component structural model: the occupation of Fe^{3+}/Al positions, the layer heights (corresponding to d_{110}) and the statistical parameters W_i , P_{ij} and M . The dependence of the lattice constant a on the fraction of the andradite component $x = \text{Fe}^{3+}/(\text{Fe}^{3+} + \text{Al})$ (Fig. 1a) and the intensity ratio between 220 and 440 reflections which is extremely sensitive to the occupation of the Fe^{3+}/Al position (Fig. 1b) were taken into account. It was found that the increase in Fe^{3+} content of 0.1 per chemical formula causes the increase in the layer height of 0.005 Å. The calculated intensities were corrected by Lorenpolarisation factor for single crystals. The comparison of the measured intensities and those calculated from the models was carried out with commonly used residual factors R_1 and R_F .

Results

Comparison of the diffraction patterns of the standard crystal and grandite samples (Fig. 2)

showed that the observed diffraction effects originate from the structure of the samples and not from the measurement conditions. The diffraction patterns of samples 1 and 2 (Fig. 3) are characterised by asymmetry and/or splitting occurring from the side of the reflections (low 2θ) and increasing along with the 2θ value (Fig. 3a,b). The reflections of sample 3 showed a rather symmetrical profile (Fig. 3c). However, in the process of modelling, extra-broadening of the reflections has been found for the diffraction patterns of samples 2 and 3. In the case of sample 2 the splitting occurs in combination with the extra-broadening, suggesting a rather complicated structure of the sample. The diffraction pattern of sample 4 (Fig. 3d) is difficult to interpret since it displays the asymmetry from low 2θ -side as well as double splitting from high 2θ -side.

The statistical parameters of the structural models which gave the best fit between the measured and calculated intensities of $hh0$ reflections of samples 1–3 are listed in Table 3. It is concluded that the inhomogeneity of grandites results from the co-existence of two types of layers, which have different Fe^{3+}/Al ratios alternating along the $[110]$ direction. The distinct feature of the interstratified structures is the strong tendency to segregation of both types of layers ($K_s = 0.97$ – 1.0) and sufficient concentration of the admixture layers ($W_2 = 0.15$ – 0.35). Since the structures are characterised by high W_2 and P_{22} values, the maximum possible thickness of a stack

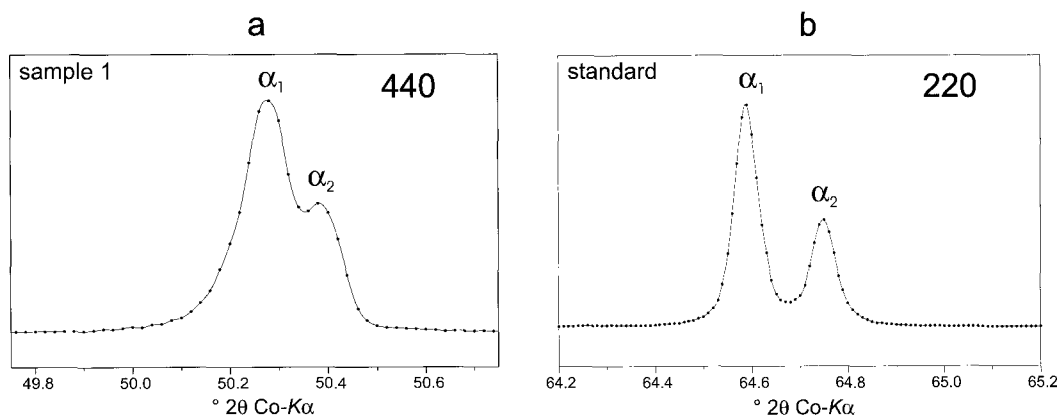


FIG. 2. The comparison of the profiles of the diffraction peaks of the sample 1 (a) and of the standard crystal of quartz (b).

of the admixture layers (the scale of inhomogeneity) is expected to be rather high — up to 500 Å. Besides, the structures of two samples (samples 2 and 3) are characterised by the fluctuations in layer heights. In sample 2, both types of layers, which show the total segregation, have variations in composition around different mean values. The structure of the sample 3 consists of only one type of layer but has a compositional variation covering nearly the whole range ($\text{Al}_{0.6-1.8}\text{Fe}_{1.4-0.2}$). The average cation composition of the crystals calculated from the models in all cases show good agreement with the data obtained independently by electron probe microanalysis of the outer zones of the samples.

We failed to find a reliable structural model which could give a good fit between the experimental and calculated diffraction patterns of sample 4. The analysis of the diffraction pattern suggests the alternation of at least four

types of layers with approximate mean x values of 0.45, 0.64, 0.76 and 0.38 respectively. This increases greatly the multivariance of modelling.

Discussion

Zonality patterns

The optical and diffraction patterns vary greatly between samples. However, there is a correlation between the optical and structural characteristics for each sample. Thus, the structure of sample 3 which is the most optically homogeneous comprises only one type of layer. The variations in Al/Fe^{3+} ratios may be in line with the existence of fine wedge-like subzones stretching nearly parallel to the (110) face.

The alternation of two types of layer, each with composition corresponding to the intermediate members of grandite series (Table 3) explains the birefringence in the outer part of sample 1. The

TABLE 3. The parameters of irregular interstratified structures of grandite crystals $\text{Ca}_3(\text{Al}, \text{Fe}^{3+})_2(\text{SiO}_4)_3$

Samp. N	$h, \text{Å}$	Cation composition of layers	Statistical parameters							Average cation composition of the outer zone	
			M	W_1	P_{ii}	K_c	$L, \text{Å}$	$l, \text{Å}$	$\sigma_h, \text{Å}$	Calculated from the model	EPMA data
1	4.210	$\text{Ca}_3(\text{Al}_{0.70}\text{Fe}_{0.30})_2$	320	0.65	0.99	0.97	1350	460	—	$\text{Ca}_3\text{Al}_{1.26}\text{Fe}_{0.74}$	$\text{Ca}_3\text{Al}_{1.32}\text{Fe}_{0.68}$
	4.225	$\text{Ca}_3(\text{Al}_{0.50}\text{Fe}_{0.50})_2$		0.35	0.98						
2	4.215	$\text{Ca}_3(\text{Al}_{0.65 \pm 0.35}\text{Fe}_{0.35 \pm 0.35})_2$	380	0.85	1.0	1.0	1600	240	0.035	$\text{Ca}_3\text{Al}_{1.24}\text{Fe}_{0.76}$	$\text{Ca}_3\text{Al}_{1.26}\text{Fe}_{0.74}$
	4.230	$\text{Ca}_3(\text{Al}_{0.45 \pm 0.35}\text{Fe}_{0.55 \pm 0.35})_2$									
3	4.210	$\text{Ca}_3(\text{Al}_{0.60 \pm 0.30}\text{Fe}_{0.30 \pm 0.30})_2$	360	1.0	1.0	—	1515	—	0.030	$\text{Ca}_3\text{Al}_{1.4}\text{Fe}_{0.6}$	$\text{Ca}_3\text{Al}_{1.4}\text{Fe}_{0.6}$

ZONALITY IN GARNETS

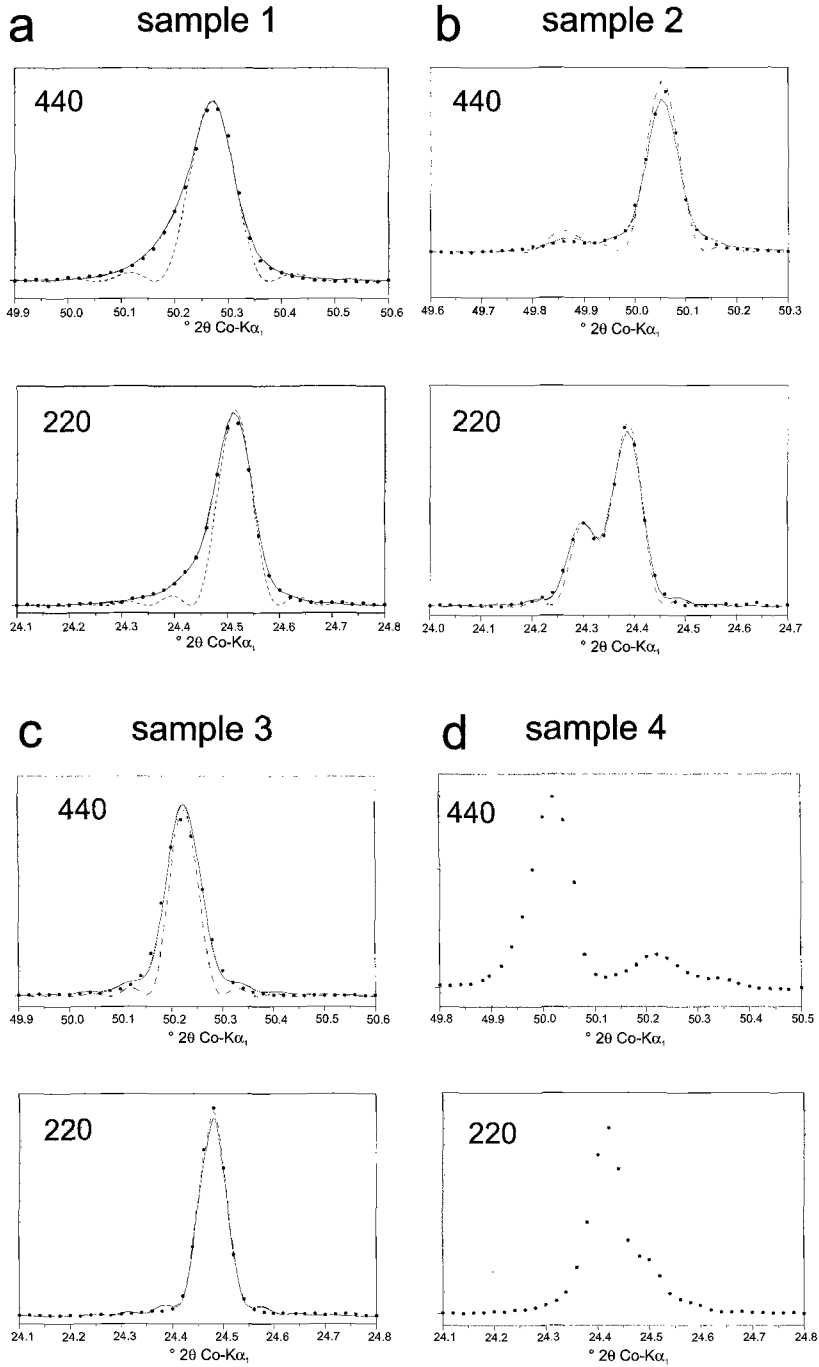


FIG. 3. (a–d) The measured intensities (dots) of $hh0$ reflections of the samples 1–4 and those calculated for the final structural models (solid line). Dashed lines represent the intensities calculated for the defect-free models (samples 1 and 3) and for the model with two types of totally segregated layers but without the fluctuations of their heights. (sample 2).

thickness of stacks of admixture layers is less than 500 Å whereas matrix layers form stacks which have thicknesses of not less than 1000 Å. These values are three orders of magnitude lower than the thickness of birefringent zones (50 µm in average), which differ in the orientation of their optical indicatrix. This means that we revealed the inhomogeneous structure of the single zone. Both of the coexisting zonalities have similar patterns but show different scales of manifestation within the sample.

The complicated structure of sample 2 contains two types of layer, both with highly variable compositions. The thickness of stacks of admixture layers is less than 200 Å whereas matrix layers form stacks of thickness not less than 1000 Å. Since the range of composition variation includes pure grossular, we may expect the occurrence of isotropic layers among the birefringent ones. A similar pattern is clearly seen in their optical properties, which indicate that the isotropic zones of 3–5 µm in thickness alternate with the birefringent zones of 10–15 µm in thickness. The outer zone of the sample contributing to the diffraction pattern is a birefringent one and it consists of alternating superfine lamellae across which the composition varies widely.

As for sample 4 the analysis of the diffraction pattern suggests the alternation of several types of layers with significantly different compositions. This is in line with the optical pattern which displays zones varying in thickness and birefringence.

Thus, the combined analysis of the results of the optical and structural studies of grandites revealed three superimposed types of zonality which are present at different scales along [110]. This conclusion is in agreement with the data published earlier (Table 1). The drastic change of structural properties from sample to sample along with the changes in their optical patterns shows evidence for the correlation between the fine and superfine oscillating zonality in grandites.

On the origin of zonality in grandites

The origin of complex multiscale zonality patterns in grandites is still questionable. Three main hypotheses have been proposed (Table 1):

1. Any compositional zonality is the result of abrupt or continuous changes in the composition of a hydrothermal solution as well as in p - T conditions occurring during crystal growth.

2. Fine growth zonality originates from the non-stationary growth dynamics.

3. Post-growth exsolution is the reason of the formation of the wave-like or tweed-like texture.

Each hypothesis is discussed separately, starting with the last, which seems to be the most unlikely.

Firstly, the occurrence of solid solution decomposition in grandites is proposed (Jamtveit, 1991) based on the absence of the crystals with certain composition of $x = 0.20$ – 0.35 and $x = 0.65$ – 0.90 . However, the published data (Table 1) and our results (Table 2) do not support this statement. Secondly, the thermodynamic solution model by Engi and Wersin (1987) suggests the existence of a miscibility gap in the range of $x = 0.02$ – 0.42 at 200°C with the solvus peak at 440°C and $x = 0.17$. On the other hand, the thermodynamic analysis by Ganguly (1976) shows a small negative deviation from ideality in the grossular–andradite join, which would prevent any immiscibility of the solid solution. Besides, the composition of the coexisting lamellae differs greatly between the data of the different authors (Table 1): $x = 0.15$ – 0.55 , 0.7 – 0.95 , 0.52 – 0.58 , 0.78 – 0.87 and 0.90 – 0.98 , that discounts the solution model of Engi and Wersin (1987). Our data on the compositions of superfine zones (Table 3) rule out the hypothesis of one or more miscibility gaps in the grandite solid solution series since the wide variations of zone compositions overlap.

Thirdly, the superposition of the lamellae with different compositions on to the growth zonality resulting in the formation of a wave-like or tweed-like texture, is considered to be the proof of the exsolution process in grandites (Hirai and Nakazawa, 1986a,b). However, Akizuki *et al.* (1984) showed that at any rate the wave-like texture could be formed during crystal growth.

It follows from the above considerations that the formation of fine oscillating zonality in grandites by solid solution decomposition is highly questionable.

The grown-in zonality can originate from the variations of growth conditions that is pointed out by the similar zonality patterns of different crystals in the same ensemble (Jamtveit *et al.*, 1995). The several scales of zonality co-existing in one and the same sample (Tables 1–3) may contradict this hypothesis. The fact that sample 2 (Table 2) is characterised by the similar fine zonality superimposed on the major zones but with a different composition, testifies to the co-

operative effect of the external conditions and the non-linear dynamics at the growth front. The particular mechanism of the latter process is discussed in only one paper (Jamtveit, 1991) where it is related to the miscibility gap in the grossular–andradite series. Even if this mechanism operates, it cannot be a general process since the oscillating zonality is peculiar for crystals with any composition. This makes the existence of a miscibility gap even more doubtful.

Most likely, the complex oscillating zonality originates from the local substance transport coupled to the surface kinetics. This mechanism is not yet elaborated in detail for the isomorphic series with perfect miscibility; however, a few models have been proposed for the zoned crystals of plagioclase (Haase *et al.*, 1980; Allegre *et al.*, 1981; Heures and Fowler, 1994). This hypothesis is consistent with the extreme abundance of the zonality in grandites of different composition as well as with the self-affinity of zoning at different scales (Tables 1–3).

Acknowledgements

This work was supported by the Russian Fund for Fundamental Investigations (projects 96-05-65579, 96-05-65577 and 95-05-14114).

References

- Akizuki, M., Nakai, H. and Suzuki, T. (1984) Origin of iridescence in grandite garnets. *Amer. Mineral.*, **69**, 896–901.
- Allegre, C.J., Provost, A. and Jaupart, C. (1981) Oscillatory zoning: a pathological case of crystal growth. *Nature*, **294**, 223–8.
- Allen, F.M. and Buseck, P.R. (1988) XRD, FTIR and TEM studies of optically anisotropic grossular garnets. *Amer. Mineral.*, **73**, 568–84.
- Drits, V.A. and Tchoubar, C. (1990) *X-ray Diffraction by Disordered Lamellar Structures*. Berlin: Springer, 371 pp.
- Engi, M. and Wersin, P. (1987) Derivation and application of a solution model for calcic garnet. *Schweiz. Mineral. Petrog. Mitt.*, **67**, 53–73.
- Frank-Kamenetskaya, O.V. and Ivanova, T.I. (1997) The modelling of irregular interstratified structures of single crystals with chemical inhomogeneity. *Cryst. Res. Technol.*, **32**, 195–211.
- Ganguly, J. (1976) The energetics of natural garnet solid solution. II. Mixing of the calcium silicate end-members. *Contrib. Mineral. Petrol.*, **55**, 81–90.
- Guinier, A. (1961) *X-ray Analysis of Crystals*. Moscow: Fizmatgiz, 604 pp. (in Russian).
- Haase, C.S., Chadam, J., Feinn, D. and Ortoleva, P. (1980) Oscillatory zoning in plagioclase feldspar. *Science*, **209**, 272–4.
- Heures, J.L. and Fowler, A.D. (1994) A non-linear model of oscillatory zoning in plagioclase. *Amer. Mineral.*, **79**, 885–91.
- Hirai, H. and Nakazawa, H. (1982) Origin of iridescence in garnet: An optical interference study. *Phys. Chem. Mineral.*, **8**, 25–8.
- Hirai, H., Sueno, S. and Nakazawa, H. (1982) A lamellar texture with chemical contrast in grandite garnet from Nevada. *Amer. Mineral.*, **67**, 1242–7.
- Hirai, H. and Nakazawa, H. (1986a) Grandite garnet from Nevada: Confirmation of origin of iridescence by electron microscopy and interpretation of a moiré-like texture. *Amer. Mineral.*, **71**, 123–6.
- Hirai, H. and Nakazawa, H. (1986b) Visualising low symmetry of a grandite garnet on precession photographs. *Amer. Mineral.*, **71**, 1210–3.
- Ivanova, T.I., Frank-Kamenetskaya, O.V., Moshkin, S.V. and Vlasov, M.Yu. (1994) The types of structural inhomogeneity of perovskite-like superconductors. *Zhurn. Strukt. Khimii*, **35**, 15–22 (in Russian).
- Jamtveit, B. (1991) Oscillatory zonation in hydrothermal grossular – andradite garnet: Non-linear dynamics in region of immiscibility. *Amer. Mineral.*, **76**, 1319–27.
- Jamtveit, B., Wogelius, R.A. and Fraser, D.G. (1993) Zonation patterns of skarn garnets: Records of hydrothermal system evolution. *Geology*, **21**, 113–6.
- Jamtveit, B., Ragnarsdottir, K.V. and Wood, B.J. (1995) On the origin of zoned grossular-andradite garnets in hydrothermal systems. *Eur. J. Mineral.*, **7**, 1339–410.
- Kingma, T. and Downs, G. (1989) Crystal-structure analysis of a birefringent andradite. *Amer. Mineral.*, **74**, 1307–16.
- Lager, G.A., Armbruster, I. and Rotella, F.G. (1989) OH substitution in garnets: X-ray and neutron diffraction, infrared, and geometric-modeling studies. *Amer. Mineral.*, **74**, 840–51.
- Lessing, P. and Standish, R.P. (1973) Zoned garnet from Crested Butte, Colorado. *Amer. Mineral.*, **58**, 840–2.
- Murad, E. (1976) Zoned, birefringent garnets from Thera Island, Santorini Group (Aegean Sea). *Mineral. Mag.*, **40**, 715–9.
- Novak, G.A. and Gibbs, G.V. (1971) The crystal chemistry of the silicate garnets. *Amer. Mineral.*, **56**, 791–823.
- Sato, M. (1965) Structure of interstratified (mixed-layer) minerals. *Nature*, **208**, 70–1.
- Shtukenberg, A.G. and Punin, Yu.O. (1996) Optical anomalies in crystals. *Zap. Vses. Mineral. Obshch.*, **125**, 104–20 (in Russian).

- Takeuchi Y., Haga, N., Umizu, S. and Sato, G. (1982) The derivate structure of silicate garnets in Grandite. *Z. Kristallogr.*, **158**, 53–99.
- Vlasova, D.K., Zharikov, V.A., Laputina, I.P. and Podlessky, K.V. (1975) Zoned garnets from skarns of Chorukh-Doiron. *Zap. Vses. Mineral. Obshch.*, **104**, 220–8 (in Russian).
- [*Manuscript received 18 August 1997: revised 29 December 1997*]